BONN-HE-2000-02
June 2000

STUDY OF DEEP INELASTIC *ep*-SCATTERING AT HIGH Q^2 WITH ZEUS AT HERA

A. KAPPES[a]
(On behalf of the ZEUS COLLABORATION)
Physikalisches Institut, Universität Bonn, Nußallee 12, D-53115 Bonn, Germany
E-mail: kappes@physik.uni-bonn.de

Measurements of differential cross sections for deep inelastic ep neutral-current (NC) and charged-current (CC) reactions are presented using data taken during the 1994–97 e^+p and the 1998–99 e^-p running periods. The structure function xF_3 has been extracted combining NC e^-p and e^+p data sets. Both the measured cross sections and xF_3 are well described by the standard model predictions using standard PDF's.

1 Introduction

During the running periods 1994–97 (e^+p) and 1998–99 (e^-p), ZEUS has collected data corresponding to integrated luminosities of $47\,\mathrm{pb}^{-1}$ and $16\,\mathrm{pb}^{-1}$, respectively. These data allow the investigation of the high-Q^2 regime both in the e^+p and the e^-p channel. For CC the new results from e^-p are compared to previously published e^+p data. For NC new results from e^-p and the extracted xF_3 points are shown. For CC e^+p (e^-p) the kinematic range is $Q^2 > 200\,\mathrm{GeV}^2$ ($Q^2 > 1\,000\,\mathrm{GeV}^2$) and for NC e^-p it is $Q^2 > 200\,\mathrm{GeV}^2$ and $0.0032 < x < 0.65$. xF_3 has been measured for $Q^2 > 3\,000\,\mathrm{GeV}^2$.

It should be noted that the center-of-mass energy has been raised from $\sqrt{s} = 300\,\mathrm{GeV}$ in 1994–97 to $\sqrt{s} = 318\,\mathrm{GeV}$ in 1998–99 by increasing the proton beam energy from $E_p = 820\,\mathrm{GeV}$ to $E_p = 920\,\mathrm{GeV}$.

2 Charged Current (CC)

To leading order, the $e^\pm p \to \text{`}\overline{\nu}\text{'}X$ cross section can be written as

$$\frac{d^2\sigma^{CC}(e^\pm p)}{dx\,dQ^2} = \frac{G_F^2}{2\pi}\left(\frac{M_W^2}{Q^2+M_W^2}\right)^2 \cdot \begin{cases} (\bar{u}+\bar{c}) + (1-y)^2\,(d+s) : e^+p \\ (u+c) + (1-y)^2\,(\bar{d}+\bar{s}) : e^-p \end{cases}, \quad (1)$$

where G_F is the Fermi constant, M_W the mass of the W boson and $\text{`}\overline{u}\text{'}$, $\text{`}\overline{d}\text{'}$, $\text{`}\overline{c}\text{'}$ and $\text{`}\overline{s}\text{'}$ are the quark momentum distributions. Measuring the high-x e^+p cross section thus mainly probes the d valence distribution, whereas e^-p mainly

[a]Supported by grants from the 'Bundesministerium für Bildung und Forschung' in Germany and the 'German-Israeli Foundation'.

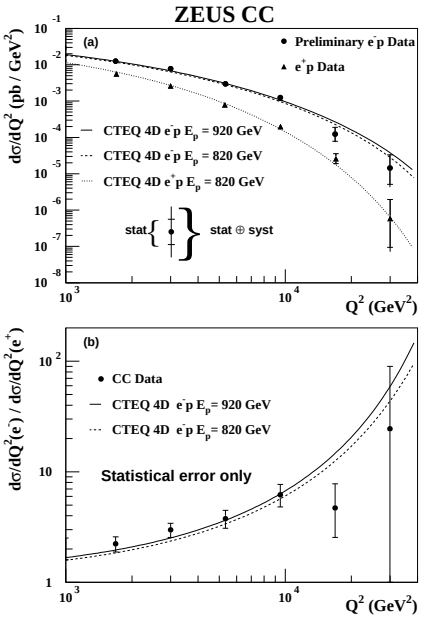

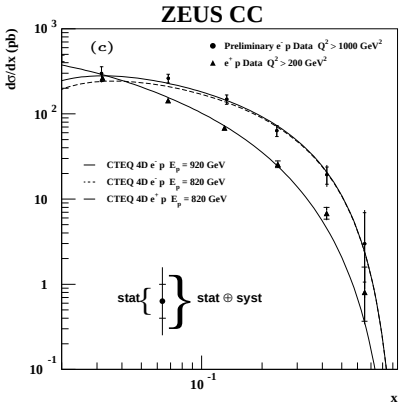

Figure 1: CC cross sections for e^+p and e^-p data. **a)**: $d\sigma/dQ^2$ vs. Q^2. **b)**: Ratio between σ_{e^-p} and σ_{e^+p}. **c)**: $d\sigma/dx$ vs. x. The solid and dotted lines show the theoretical predictions using CTEQ4D [3]. The dashed lines are the theoretical predictions for e^-p at $E_p = 820\,\text{GeV}$.

carries information on the u valence distribution. In contrast to e^-p scattering, for e^+p the valence contribution to the cross section is suppressed by the factor $(1-y)^2$.

The single differential cross sections $d\sigma/dQ^2$ for e^-p [1] and e^+p [2] are shown as functions of Q^2 in Fig. 1a. Figure 1b shows the ratio between the two cross sections. The increase in the cross section by more than an order of magnitude when switching from e^+p to e^-p for $Q^2 \gtrsim 10\,000\,\text{GeV}^2$ is evident. It is mainly due to the higher u quark content of the proton wrt. its d quark content and the additional suppression of the d quark distribution in the e^+p case. Only a small fraction of the increase originates from the increased proton beam energy. The Q^2 dependence of the propagator term in Eq. 1 permits the determination of the W mass from a fit (not shown) to the measured $d\sigma/dQ^2$ points [2]. Fixing G_F to the SM value yields $M_W = 81.4^{+2.7}_{-2.6}(\text{stat.}) \pm 2.0(\text{syst.})^{+3.3}_{-3.0}(\text{PDF})$ GeV, which is compatible with the world average. Note that in ep scattering space-like W's are exchanged whereas e.g. at Tevatron or LEP the W's are produced on-shell.

Figure 1c shows $d\sigma/dx$ versus x for e^-p and e^+p. Note that in the case of e^+p the data are for $Q^2 > 200\,\text{GeV}^2$, whereas for e^-p the region $Q^2 > 1\,000\,\text{GeV}^2$ was selected. Nevertheless, for $x > 0.04$ the e^-p cross section exceeds the e^+p cross section. The errors on the measured cross sections are

large in the high-x range and of the same order of magnitude as the uncertainties of the theoretical predictions (not shown). Hence the data can not yet contribute to an improvement of the uncertainties of the PDF's in this region.

3 Neutral Current (NC)

To leading order, the NC cross section can be written as

$$\frac{d^2\sigma^{NC}\,(e^{\pm}p)}{dx\,dQ^2} = \frac{2\pi\alpha^2}{x\,Q^4}\left[Y_+ F_2^{NC} \mp Y_- xF_3^{NC} - y^2 F_L^{NC}\right] , \qquad (2)$$

where $Y_\pm = 1 \pm (1-y)^2$. In contrast to the charged current case, the exchanged boson couples to all quark flavors, yielding the structure functions

$$F_2 = x\sum_f A_f \cdot [q_f + \bar{q}_f] \qquad xF_3 = x\sum_f B_f \cdot [q_f - \bar{q}_f] \ , \qquad (3)$$

where the sum runs over the different quark flavors f, A_f and B_f are the electroweak coupling factors and '$\overline{q}$' are the quark momentum distributions. The contribution of the longitudinal structure function F_L can be neglected for the selected kinematic range. For $Q^2 \ll M_Z^2$ (M_Z being the Z mass), also the contribution of xF_3 to the cross section can be neglected. However, for $Q^2 \gtrsim M_Z^2$ the weak and electromagnetic forces become comparable in size, implying a sizable contribution of xF_3.

Figure 2 shows the e^-p reduced cross section $\tilde{\sigma} = \frac{d^2\sigma^{NC}}{dx\,dQ^2} \cdot \frac{x\,Q^4}{2\pi\alpha^2}\frac{1}{Y_+}$ as a function of Q^2 at fixed values of x ranging from 0.65 down to 0.0032. Both the CTEQ4D [3] and MRST(99) [4] parameterizations describe the data well over the whole x range. The cross section is dominated by F_2 at low Q^2, where scaling violation is driven by QCD, whereas at high Q^2 the xF_3 contribution becomes significant and causes an increase in the cross section.

xF_3 has been determined from the difference of e^-p and e^+p [5] cross sections using $16\,\mathrm{pb}^{-1}$ of e^-p data ($\sqrt{s} = 318\,\mathrm{GeV}$) and $30\,\mathrm{pb}^{-1}$ of e^+p data ($\sqrt{s} = 300\,\mathrm{GeV}$). Figure 3 shows the extracted xF_3 versus x for five values of Q^2 ranging from $3\,000\,\mathrm{GeV}^2$ up to $30\,000\,\mathrm{GeV}^2$. Comparing the sizes of the statistical errors to the F_L contributions (corrections to the calculated xF_3 arising from different $\sqrt{s}$ values of the two data sets), calculated from CTEQ4D, justifies the assumption $F_L = 0$. The two theoretical predictions from CTEQ4D and MRST(99) are very similar and both describe the data well.

4 Summary

$47\,\mathrm{pb}^{-1}$ of e^+p and $16\,\mathrm{pb}^{-1}$ of e^-p data have been analysed to obtain high-Q^2 NC and CC cross sections. The CC cross sections $d\sigma/dQ^2$ and $d\sigma/dx$ have been

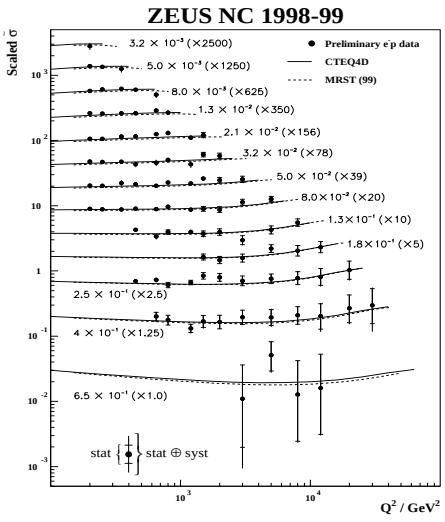

Figure 2: Reduced cross section $\tilde{\sigma}$ versus Q^2 for fixed values of x (e^-p data). The cross sections of each x bin are scaled by the factor in parentheses. The solid and dashed lines show the theoretical predictions using CTEQ4D and MRST(99) [4], respectively.

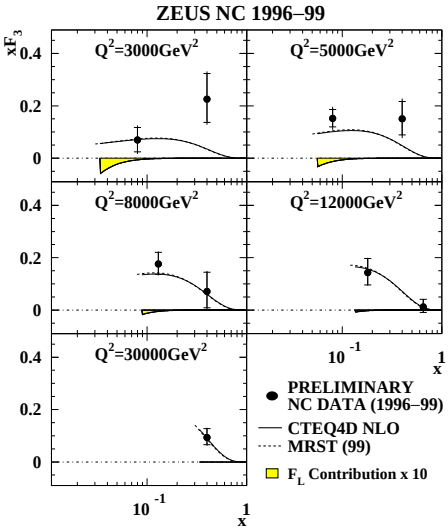

Figure 3: xF_3 versus x for fixed values of Q^2 from the combined e^+p and e^-p data sets. The solid and dashed lines show the theoretical predictions using CTEQ4D and MRST(99), respectively. The shaded band in each Q^2 bin indicates the F_L contribution multiplied by a factor of 10.

measured for $Q^2 > 1\,000\,\mathrm{GeV}^2$ (e^-p) and $Q^2 > 200\,\mathrm{GeV}^2$ (e^+p), respectively. The e^-p NC cross section $d^2\sigma/dx\,dQ^2$ has been determined for $Q^2 > 200\,\mathrm{GeV}^2$ and $0.0032 < x < 0.65$. Combining the e^+p and e^-p data sets made it possible to extract the structure function xF_3 for the first time in the high-Q^2 regime, $Q^2 > 3\,000\,\mathrm{GeV}^2$. All measured cross sections and xF_3 are well described by the standard model predictions using standard PDF's.

References

1. ZEUS Collab., J. Breitweg et al., Measurement of High-Q^2 Charged-Current e^-p Deep Inelastic Scattering Cross Sections, contributed paper #558 to ICHEP99, Tampere (1999).
2. ZEUS Collab., J. Breitweg et al., *Eur. Phys. J.* C **12**, 411 (2000).
3. H.-L. Lai et al., *Phys. Rev.* D **55**, 1280 (1997).
4. A.D. Martin et al., *Nucl. Phys. Proc. Suppl.* **79**, 105 (1999).
5. N. Tuning, these proceedings.